UNIVERSITY OF ZIELONA GÓRA

CIVIL AND ENVIRONMENTAL ENGINEERING REPORTS

E-ISSN 2450-8594

CEER 2024; 34 (3): 0136-0153
DOI: 10.59440/ceer/190880
Original Research Article

GLASS BEAMS USED IN STEEL-GLASS ROOFS FOR THE ADAPTIVE REUSE OF HISTORIC BUILDINGS

Anna JÓŹWIK[1]
Warsaw Univerity of Technology, Faculty of Architecture, Warsaw, Poland

A b s t r a c t

This article concerns the use of structural glass in the adaptive reuse of historic facilities using glass beams as structural elements in steel-glass roofs. More and more often, glass is increasingly being used as a structural material. This fact provides new design possibilities in the adaptation of historic buildings due to the neutral perception of glass and, at the same time, offers the possibility of distinguishing modern structural elements in the historic fabric. The use of structural glass is, however, associated with limited spans of structural elements. For larger spans, solutions of mixed materials are proposed, which are exemplified by steel-glass roofings. Based on selected examples, steel-glass systems with the use of glass beams are characterised. The strength of glass as a structural material is discussed. The main approaches in the design of glass beams with the lateral-torsional buckling phenomenon are indicated.

Keywords: structural glass, glass structures, glass beams, steel-glass roofs, lateral-torsional buckling, adaptive reuse of historic buildings

1. INTRODUCTION

Nowadays, the preservation of built cultural heritage represents a significant design challenge. Adaptive reuse is one of the recognised strategies aimed at preserving historic buildings [1–6]. No clear definition of the term adaptive reuse has yet been made, as noted by various researchers [5, 7]. Nevertheless, considerations of the definition of adaptive reuse can be found in numerous publications. Wilkinson et al. [8] and Vafaie at al. [9] note that a huge number of terms, such as renovation, refurbishment, remodeling, reinstatement, retrofitting, conversion, transformation, rehabilitation, modernisation, re-lifing, restoration are used to define adaptation. According to ICOMOS [10], a successful adaptation project modifies a site, or a building, for its use while preserving its heritage value. It has been explicitly stated that adaptation should not dominate or significantly obscure the original form or material, and should not adversely affect the shaping of a site that constitutes a valuable cultural heritage. Plevoets

[1] Corresponding author: Warsaw University of Technology, Faculty of Architecture,, ul. Koszykowa 55, 00-659 Warszawa, Poland, anna.jozwik@pw.edu.pl

and Van Cleempoel state clearly that the term adaptive reuse refers to changes involving a functional and physical element. A change in function does not necessarily imply a radical change; it may be more subtle [5]. This is related to the redevelopment of existing buildings for new or continued use, which may lead to a complete change or be limited to minor changes [5]. Douglas, on the other hand, focuses on the technical aspect, understood as any construction work beyond maintenance to change capacity, function or performance [11]. The technical aspect was also distinguished by Plevoets and Van Cleempoel, who identified three different approaches to adaptive reuse: 1) typological, 2) technical and 3) architectural strategies [12, 13].

Glass can be used as a building and construction material in architectural concepts aimed at reusing a heritage building [14–18]. Various architectural concepts are being developed that enable changing the function or improving the conditions of the building use. As part of the adaptation of historic buildings, solutions are presented in which a glazed roofing is proposed. Jäger [19] classified the strategy adopted towards the existing fabric as 1) addition, 2) transformation, 3) conversion. With glazed roofing, within the strategies mentioned, additional usable space is quite often gained, which offers a significant benefit of such solutions. Glazing also allows light to enter the building, while at the same time allowing to distinguish between new and old building development and exposing the view of historic building development. It is now possible to design all-glass roof structures but with limited spans [16, 17]. Examples of such structures include the V&A Museum in London, the Town Library in Enfield, Family Home of John Paul II in Wadowice. In all-glass roofs, laminated glass beams are most commonly applied as the main load-bearing elements. For larger spans, a need emerges for steel structures, which can be designed in various structural systems. Steel-framed glazed roofs have been designed for numerous historic facilities, such as the British Museum in London, the Reichstag Dome in Berlin and the Central Train Station in Strasbourg. In addition to all-glass roofs and steel roofs, steel-glass roof roofings with mixed material solutions can be distinguished. The main load-bearing elements are designed of steel, while glass beams constitute the second-order elements. These beams act as purlins supporting the glass panels. Such solutions are far from common; thus the lack of studies on the ways to design steel-glass roofs with the use of glass beams.

The purpose of the following article is to present the potential for the use of structural glass in adaptive reuse. This issue remains under-recognised, despite the design opportunities offered by the use of structural and building glass in historic buildings. The scope of the analysis concerns steel-glass roofing with the use of glass beams. The development of glass structures is facilitated by an increase in knowledge of the mechanical and strength-related properties of glass, although the inadequate availability of design methods and procedures still needs to be noted. This also concerns the design of glass beams. Works are underway on normative documents with regards to the design of structural glass, including glass beams, which will result in Eurocode 10 [20, 21].

2. THE PROPERTIES OF GLASS AS A STRUCTURAL MATERIAL

2.1 Mechanical and strength properties of glass

In assessing the feasibility of glass being used as a construction material, its mechanical and strength-related properties play an important role. One of the basic mechanical properties of glass is its Young's modulus, which stands at 70 000 MPa, the same as for aluminium. In comparison, Young's modulus for steel is 210 000 MPa. In addition to Young's modulus, Poisson's ratio can be compared, which stands at 0.23 for glass and 0.3 for aluminium and steel. Table 1 below compares the physical and mechanical properties of glass as compared to aluminium and steel.

Table 1. Physical and mechanical properties of basic soda lime silicate glass and steel [22–24]

Material / Properties	Symbol	Unit	Soda lime silicate glass	Aluminium	Steel
Density	ρ	kg/m^3	2 500	2 700	7 850
Young`s modulus	E	MPa	70 000	70 000	210 000
Poisson`s ratio	ν	-	0.23	0.3	0.3
Shear modulus $G = \frac{E}{2(1+\nu)}$	G	MPa	24 455	27 000	81 000
Coefficient of linear thermal expansion	α_t	$°C^{-1}$	$9 \cdot 10^{-6}$	$26 \cdot 10^{-6}$	$12 \cdot 10^{-6}$

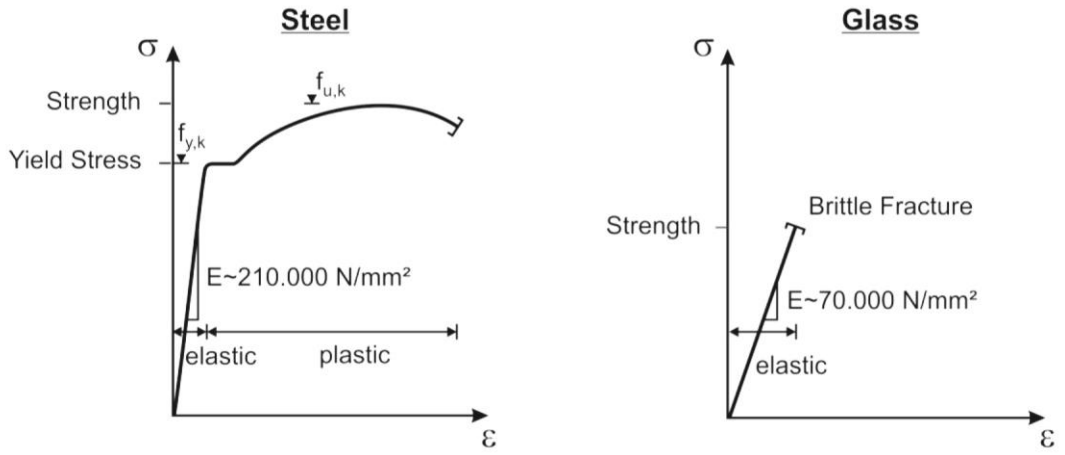

Fig. 1. Stress-strain relations of steel and glass [25]

The theoretical strength of glass is quite high. In the case of tensile strength, the strength of glass can reach 32 GPa, which results from interatomic bonds [26]. In practice, however, the strength of glass is significantly lower. The reduction in glass strength is influenced by such aspects as structural defects. According to Grifitth's theory [27], cracks in glass are the cause of stress concentration. Compared to steel, glass is a brittle material (Figure 1); thus, plastic distribution of stresses concentrated in the fracture areas of glass sheets is impossible. This leads to sudden damage to the glass. Therefore, the strength of glass is determined by several factors, including the size of the cracks or the surface condition of the glass panel. In practice, the characteristic bending strength value for annealed float glass is 45 MPa [22]. Higher glass strengths are achievable if a thermal treatment process is applied. By deliberate heating of glass to a temperature close to its softening point and then by slow cooling, heat-strengthened glass with a strength of 70 MPa (Table 2) is obtained, whereas rapid cooling leads to obtaining thermally toughened glass with a strength of 120 MPa (Table 2). In special cases, the strength of the glass can be increased by chemical processes. The characteristic strength of chemically strengthened glass can be 150 MPa (Table 2). The thermal and chemical treatment process also affects the nature of the crack network and

the size of the glass fragments in the event of its breakage [20]. This is important for the classification of glass as safety glass.

Table 2. Values of characteristic bending strength $f_{b,k}$ for design of prestressed basic soda lime silicate glass

Glass material	Values for characteristic strength $f_{b,k}$ from-stressed glass processed from:		
	Thermally toughened safety glass to EN 12150-1 [28] and heat-soaked thermally toughened safety glass to EN 14179-1 [29]	Heat-strengthened glass to EN 1863-1 [30]	Chemically strengthened glass to EN 12337-1 [31]
float glass or drawn sheet glass	120 MPa	70 MPa	150 MPa

For design purposes, at the ultimate limit state, the calculative bending strength of the glass is determined according to the formula given in Technical Specification CEN/TS 19100:2021 [32]:

$$f_{g,d} = k_e \cdot k_{sp} \cdot \lambda_A \cdot \lambda_l \cdot k_{mod} \cdot \frac{f_{g,k}}{\gamma_M} + k_p \cdot k_{e,p} \cdot \frac{f_{b,k} - f_{g,k}}{\gamma_p}, \quad (2.1)$$

where:
$f_{g,k}$ – the characteristic value of bending strength for annealed glass,
$f_{b,k}$ – the characteristic value of bending strength after a strengthening treatment,
γ_M – material partial factor, depends on the class of consequences, for glass beams CC2 [33] $\gamma_M = 1.8$,
γ_p – partial factor for prestress on the surface, depends on the class consequences, for the CC2 $\gamma_p = 1.2$,
k_e – edge or hole finishing factor, for float annealed glass with polished edges k_e=1.0,
k_{sp} – surface treatment factor, for float glass $k_{sp} = 1.0$,
λ_A – size-effect factor area, for area ≤18 m^2 $\lambda_A = 1.0$,
λ_l – size-effect factor length (edge, hole), for length ≤6.0 m $\lambda_l = 1.0$,
k_{mod} – modification coefficient depending on load duration,
k_p – coefficient accounting for the reduction of the process-inducted prestressed, for float glass and polished edges k_p=1.0,
$k_{e,p}$ – edge or hole prestressing factor, for heat strengthened and thermally toughened (in-plane loading in case of beams) $k_{e,p}$=1.0.

In the formula (2.1) used to determine the calculative bending strength of glass $f_{g,d}$, partial safety coefficients have been introduced, in accordance with the limit state design that will be in force under Eurocode 10 [20]. One of these is the modification coefficient k_{mod}. Its value depends on the duration of the load; for typical loads, it ranges from 0.29 to 1.0. A k_{mod} value of 1.0 is assumed for short-term loads, e.g. wind gusts. For long-term loads, the value of the coefficient is lower; for permanent loads, it stands at 0.29. This means that the calculative load value of glass for bending varies according to the type of load and its duration. When different types of loads operate, it is advisable that for further

calculations, the load with the shortest duration or a weighted average that takes into account combinations of loads of various durations is considered [34].

2.1. Structural behaviour of laminated glass

In theoretical analyses, the structural behaviour of a monolithic glass beam is often considered. However, in design practice, laminated glass beams are used as a result of the requirement to ensure a certain level of safety. Laminated glass is obtained by glueing together two or more layers of glass panes joined by special adhesive layers. The glass lamination process takes place in an autoclave at a temperature of approximately 120°C and at a pressure of 12 bar [35]. The materials used for glass lamination include polyvinyl butyral (PVB) film or its stiffer variant at thicknesses of 0.38, 0.76, 1.52, and 2.25 mm. This material is an amorphous thermoplastic that adheres to the glass through hydrogen bonds [36]. In solutions with special design requirements, SentryGlas ionomer is quite often used. Similarly to the PVB film, the ionomer is a viscoelastic material whose stiffness depends on the duration of load and the operation temperature. It is characterised by a significantly higher stiffness and less sensitivity to load duration and operation temperature, as compared to other interlayers [37]. Additionally, SentryGlas ionomer exhibits high tensile strength and five times the tear strength, as compared to a typical PVB film [20].

Laminated glass exhibits residual load capacity in the event of breakage of one of the glass layers [38, 39]. Following a breakage, the adhesive layers hold the glass fragments and thus a post-breakage strength is achievable; this depends on the type of glass used. The larger the shards of the broken glass, the higher its post-breakage strength. The largest glass fragments are obtained after breaking annealed float glass, then for heat-strengthened glass. Thermally toughened glass has the lowest post-breakage load capacity, although it has a higher load capacity and impact resistance than annealed float glass and heat-strengthened glass [26].

The post-breakage behaviour of laminated glass is important with regard to its use as a structural material and was therefore researched by Bennison et al. [40] and Kott [41]. The mechanism of failure of laminated glass at bending has been analysed based on a model of a glass plate consisting of two panes of glass bonded by a PVB film. Kott [41] distinguished three stages of operation (Figure 2). In stage I, the glass sheets remain undamaged. The cooperation of the glass sheets is based on the sandwich theory [42], namely, the distribution of compressive and tensile stresses depends on the value of the shear modulus of the interlayer in the laminated glass. In stage II, one of the glass panes breaks and then the tensile stresses are mainly, or fully, taken over by the unbroken glass sheet. In stage III, both panes of glass are damaged in the same cross-section. The compressive stresses can then still be transferred between the pieces of broken glass, while the tensile stresses are taken over by the interlayer only. Excessive elongation or tearing of the interlayer leads to complete destruction of the glass.

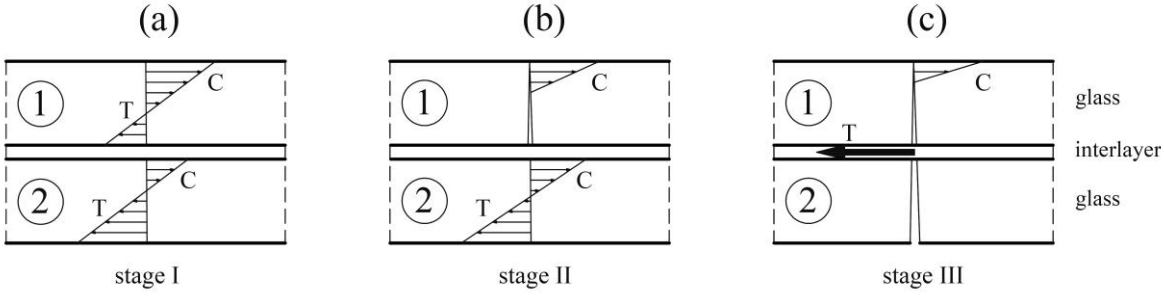

Fig. 2. Three stages in the failure process of laminated glass: (a) stage I; (b) stage II; (c) stage III. Figure adapted from [20]

3. LATERAL-TORSIONAL BUCKLING OF LAMINATED GLASS BEAMS

3.1. Design buckling curves for laminated glass beams

Lateral torsional buckling poses a significant problem in the design of flexural beams. Many researchers undertake analytical, numerical and experimental studies [43–50] to research this phenomenon for the purpose of using glass as a structural material. Glass beams are characterised by their high slenderness ratio, which results from the proportion of the cross-sectional dimensions relative to their span. For this reason, elements subjected to bending are susceptible to buckling in the compression zone. For steel, timber or concrete beams, buckling and instability are prevented by using appropriate design methods. Typically, standardised buckling curves are used. This approach has also been adopted for the design of steel columns and beams in the design standard Eurocode 3 [24]; according to its guidelines, the resulting design moment M_{Ed} should not exceed the value of the design moment buckling strength $M_{b,Rd}$.

$$M_{Ed} \leq M_{b,Rd} = \chi_{LT} \cdot W_y \cdot \frac{f_{yk}}{\gamma_{M1}}, \tag{3.1}$$

where:
χ_{LT} – reduction factor for lateral-torsional buckling,
W_y – section modulus about the strong axis of the beam,
f_{yk} – characteristic value of yield strength,
γ_{M1} – partial safety factor.

The resistance is of a beam with the account of buckling $M_{b,Rd}$ is expressed using the buckling reduction factor χ_{LT}, the value of which can be determined using the following equation:

$$\chi_{LT} = \frac{1}{\Phi_{LT} + \sqrt{\Phi_{LT}^2 - \bar{\lambda}_{LT}^2}}, \chi_{LT} \leq 1.0, \tag{3.2}$$

with:

$$\Phi_{LT} = 0{,}5 \cdot [1 + \alpha_{imp} \cdot (\bar{\lambda}_{LT} - \alpha_0) + \bar{\lambda}_{LT}^2], \tag{3.3}$$

$$\bar{\lambda}_{LT} = \sqrt{\frac{M_{pl}}{M_{cr}^{(E)}}} = \sqrt{\frac{W_y \cdot \sigma_{yk}}{M_{cr}^{(E)}}}, \tag{3.4}$$

where:
Φ_{LT} – buckling reduction factor,
$\bar{\lambda}_{LT}$ – slenderness ratio for lateral-torsional buckling,
α_{imp}, α_0 – imperfection factors,
$M_{cr}^{(E)}$ – elastic critical moment for lateral-torsional buckling,
M_{pl} – plastic moment resistance,
σ_{yk} – yield stress.

The method for considering lateral-torsional buckling in the design of glass beams has been adapted from Eurocode 3 [24] and is presented in numerous papers [43–46, 49]. The determination of the buckling curve together with the imperfection factors poses a problematic issue. In the works by Lubile

and Crisinel [43–45], a design curve 'c' is assumed with imperfection factors α_{imp}=0.45 and α_0=0.20 according to Eurocode 3 [24]. In the Guide for the Design, Construction and Control of Buildings with Structural Glass Elements CNR-DT 210/2013 [51], the factors with the following values: α_{imp}=0.26 and α_0=0.20 are taken from a study by Bedon and Amadio. According to a study by Ferreira [52], the more suitable values for the imperfection factors stand at α_{imp}=0.35 and α_0=0.00.

For buckling curves, the slenderness ratio $\bar{\lambda}_{LT}$ and the reduction factor χ_{LT} are determined similarly as for steel beams. However, in contrast to steel, both values are based on tensile strength [43–45], thus the slenderness ratio for lateral-torsional buckling $\bar{\lambda}_{LT}$ is determined as follows:

$$\bar{\lambda}_{LT} = \sqrt{\frac{\sigma_{Rk}}{M_{cr}^{(E)}}} = \sqrt{\frac{2 \cdot \sigma_{Rk} \cdot W_y}{M_{cr}^{(E)}}}, \tag{3.5}$$

Where:
σ_{Rk} – characteristic tensile strength of glass,
$M_{cr}^{(E)}$ – elastic critical lateral-torsional buckling.

The reduction factor χ_{LT} is determined in the slenderness ratio function $\bar{\lambda}_{LT}$ as:

$$\chi_{LT} = f(\bar{\lambda}_{LT}) \tag{3.6}$$

Hence the design value of the bending moment capacity $M_{b,Rd}$ is:

$$M_{b,Rd} = \chi_{LT} \cdot \sigma_{Rd} \cdot W_y, \tag{3.7}$$

where:
σ_{Rd} – design tensile strength of glass,
W_y – section modulus about the strong y-axis of the beam.

3.2. Elastic critical moment for lateral-torsional buckling of laminated glass beams

3.2.1. Lateral-torsional buckling for laterally unrestrained glass beams

In the design of glass beams, the value of the elastic critical moment $M_{cr}^{(E)}$ is used to determine the slenderness ratio for lateral-torsional buckling $\bar{\lambda}_{LT}$. One of the first approaches to determining the elastic critical moment $M_{cr}^{(E)}$ was presented in the work by Lubile and Crisinel [43–45]. The method can be applied to both monolithic and laminated glass beams. The beam is assumed to be supported by fork supports and loaded with a constant moment load with the top edge being unsupported (Figure 3).

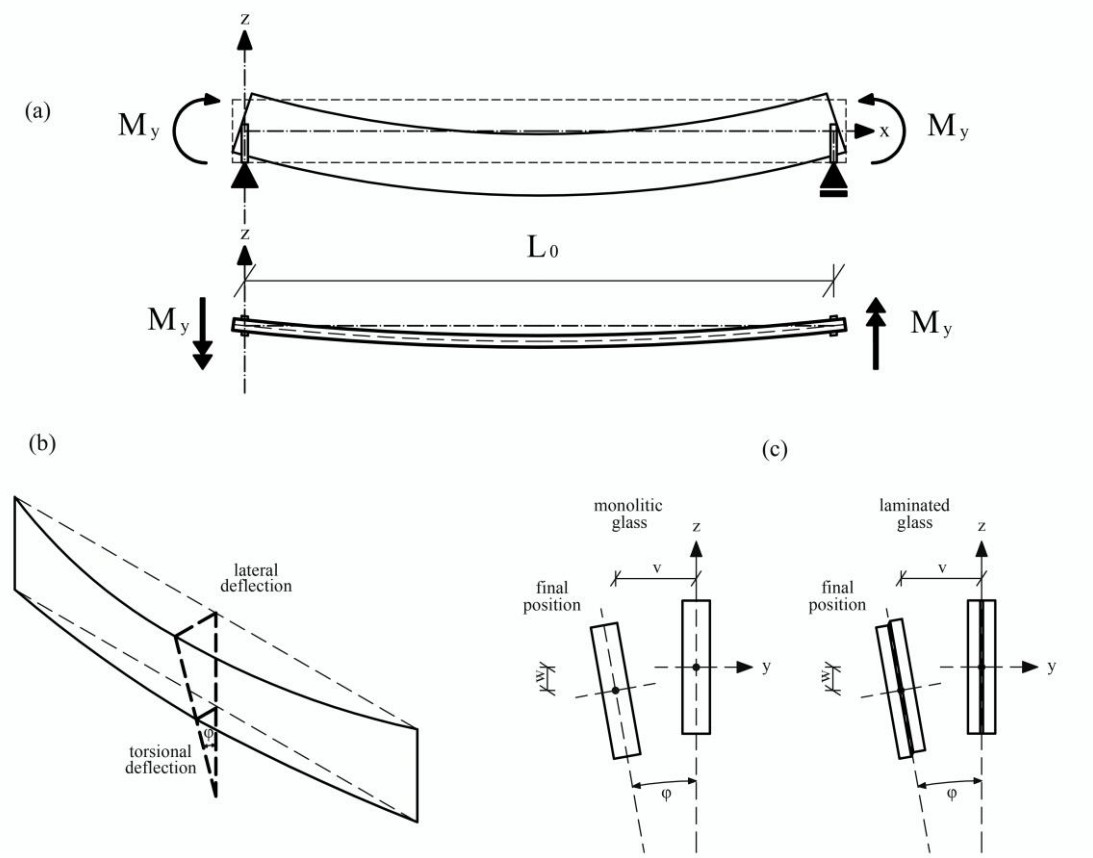

Fig. 3. Lateral-torsional buckling of a simply supported beam: (a) overview; (b) deformation of beam; (c) cross-section deformation for monolithic and laminated glass. Figures adapted from [46, 50]

For such assumptions, the critical torsional buckling moment of a beam with a rectangular cross-section can be calculated for with:

$$M_{cr} = C_1 \cdot \frac{\pi^2 \cdot E \cdot I_z}{L_{cr}^2} \left[\sqrt{C_2 \cdot z_a + \frac{G \cdot K \cdot L_{cr}^2}{\pi^2 \cdot E \cdot I_z}} + C_2 \cdot z_a \right], \tag{3.8}$$

where:
E – Young`s modulus for glass,
I_z – moment of inertia about the minor z-axis of the beam,
G – shear modulus,
K– torsion constant,
L_{cr} – buckling length,
C_1 – factor depends on different bending moments (table 3),
C_2 – factor depends on different bending moments (table 3),
z_a – distance between the centre of gravity and the point where the load is applied.

Table 3. Lateral-torsional buckling factors C_1 and C_2 [26]

Bending moment	C_1	C_2
Constant	1.0	-
Linear (zero at mid span)	2.7	-
Parabolic (zero at both extremities)	1.13	0.46
Triangular (zero at both extremities)	1.36	0.55

3.2.2. Lateral-torsional buckling for laterally restrained glass beams

Glass beams are used in roofs to support glass panels using mechanical or adhesive connections. These connections are characterised by stiffness that reduces susceptibility to displacement along the top edge of the beam either continuously or in discrete locations. Nowadays, a growing body of research is focused on silicone connections, which can be considered as additional flexible supports (Figure 4).

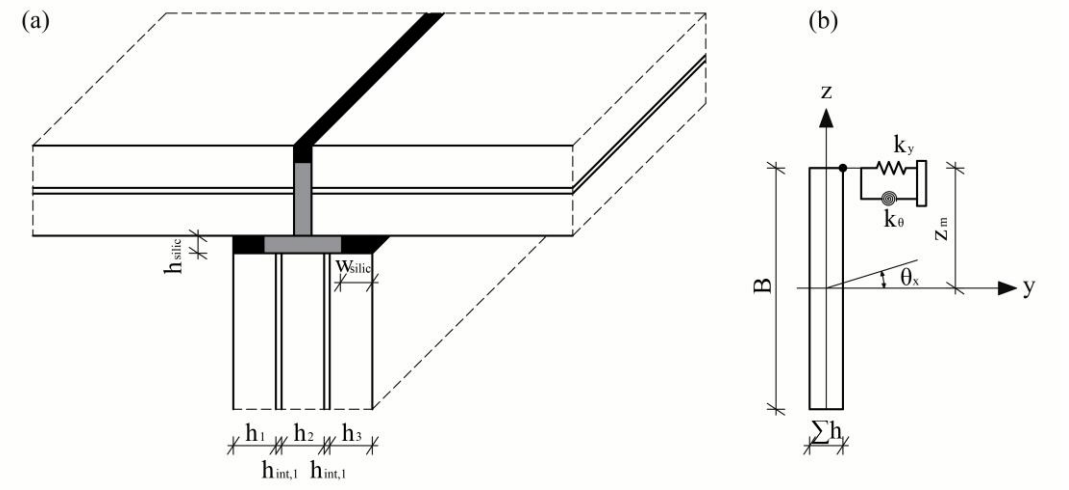

Fig. 4. Laminated glass beam with continuous silicone joints: (a) overall view; (b) analytical model of cross-section. In the figure: k_y – represents the translational (shear) rigidity of the continuous elastic restraint, per unit of length, along the y-axis; k_y – is the rotational rigidity of the continuous elastic restraint, per unit of length, about the x-axis. Figure adapted from [53]

Numerous publications that present research results show the advantageous effect of lateral restraints. [53–59]. Belis and Bedon [53] analysed the critical buckling moment of simply supported beams and restrained laterally along their top edge. Significantly, the analytical critical moment values obtained matched reasonably well with those obtained in the numerical analyses, but in later work conducted by Bedon and Amadio [54] the matching of the results was even better. Bedon and Amadio [54] also studied the elastic buckling behaviour of monolithic glass beams with an elastically restrained edge (Figure 4). A closed-form expression was derived for the critical buckling load of a beam loaded by a uniform bending moment, taking into account that the number of half-sine waves n_R in the buckling shape can be greater than one (Figure 5). For such beams with a rectangular section (for the rotational stiffness of the continuous elastic restraint $k_\theta = 0$ and $I_\omega = 0$ the warping constant), the critical moment can be calculated as:

$$M_{cr,R}^{(E)} = M_{cr,R} = z_M \cdot k_y \cdot \left(\frac{L_0}{n_R \cdot \pi}\right)^2 \pm \sqrt{\left[E \cdot I_z \cdot \left(\frac{n_R \cdot \pi}{L_0}\right)^2 + k_y \cdot \left(\frac{L_0}{n_R \cdot \pi}\right)^2\right] [G \cdot I_z + z_M^2 \cdot k_y \cdot \left(\frac{L_0}{n_R \cdot \pi}\right)^2]}, \quad (3.9)$$

where:
z_M – distance between the continuous lateral restraint and the x-axis,
k_y – joint shear rigidity,
n_R – number of half-sine waves able to minimize,
E – Young`s modulus,
G – shear modulus,
I_z – moment of inertia about the minor z-axis of the beam,
L_0 – buckling length.

In accordance with equation (3.9), for a monolithic glass beam subjected to a constant bending moment M_y, it can be also indicated that:
- in presence of a 'weak' sealant joint ($k_y = 0$), $n_R = 1$, the critical buckling moment is:

$$M_{cr,R}^{(E)} = M_{cr}^{(E)}, \quad (3.10)$$

where $M_{cr}^{(E)} = \frac{\pi}{L_0} \cdot \sqrt{EI_z \cdot GI_t}$, in this equation E and G represent Young`s and shear moduli of glass, while I_z signifies the moment of inertia about minor z-axis and I_t is the torsional moment of inertia;
- in presence of a partially rigid sealant joint ($0 < k_y < \infty$), $n_R > 1$, the critical buckling moment is:

$$M_{cr,R}^{(E)} = R_M \cdot M_{cr}^{(E)}, \quad (3.11)$$

where: $R_M = f(k_y,\ B,\ h,\ L_0,\ z_M,\ n_R) > 1$ is amplification factor able to take into account the effects driving from the joint shear rigidity k_y geometrical condition of the beam, the glass elastic bending and torsional stiffnesses, also the position of the applied restraints z_M and the half sine-waves n_R able to minimize, base on equation (3.9).

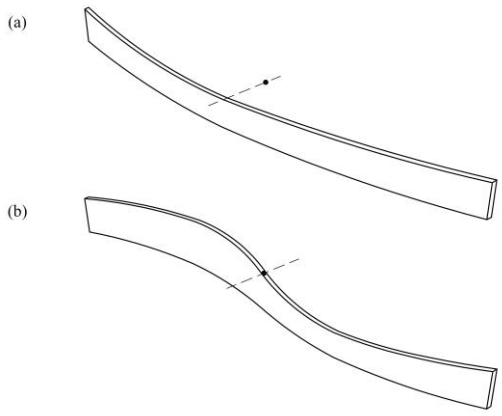

Fig. 5. Lateral-torsional buckling deformed shape for a laminated glass beam with lateral restraints: (a) number of half-sine waves n_R=1; (b) number of half-sine waves n_R=2

4. STEEL-GLASS ROOFS WITH GLASS BEAMS

4.1. General characteristics

The structural solutions for roofing that are used in the adaptive reuse of historic buildings include steel-glass roofs with glass beams. The combination of the two construction materials makes it possible to obtain structurally and functionally efficient load-bearing systems. The choice of structural solution for the roof depends on such aspects as the horizontal span, the geometric form of the roof, the shape of the roof plan and the layout of supports [60]. Steel-glass beam systems can be formed using the main steel elements in the form of:

- beams,
- frames,
- trusses,
- cable girders.

The cross-sections of the steel elements are designed from both hot-rolled profiles and plate girder profiles, as well as specially formed cross-sections in the shape of triangles, trapezoids, etc. The initial height of the cross-section in steel beams is assumed as 1/25 of the span L, while in frame rafters it is assumed as 1/30-1/40. Steel trusses can be characterised by different shapes and truss patterns [61]. The height of the truss depends on the shape; for double-trapezoidal trusses and those with parallel strips, the height can be assumed as 1/8-1/12 of its span L [62]. Cable girders can be shaped using only steel tendons, an example of which is the Jawerth system [63, 64], or as a hybrid string structure [65]. The height of the cable girders should be selected using the $H \geq L/8$ condition [64]. Cable trusses with parallel chords with full x-shaped trussing are a special type of cable girders. This pattern of truss contributes to reducing the tension force [64].

In steel-glass roofing, the glass beams act as purlins. By using structural glass, the proportion of steel structural elements can be reduced, which is advantageous in the design of historic buildings. Glass beams are designed as multi-layered laminated glass. The initial cross-sectional height can be assumed as 1/17 L [66]. The beams are supported on the main structural elements by welded steel ‘shoes’. When developing structural details of glass, it is crucial to avoid stress concentrations and direct contact between steel and glass. For this reason, liners such as polyoxymethylene (POM) [26, 66] are used in steel ‘shoes’.

The spacing of the glass beams is correlated with the dimensions of the glass roof panels and equals approximately 1.5÷2.0 m. Insulated glass units (IGU) are most commonly used on roofs. Due to the nature of the glazing placed above the heads of facility users, it is advisable to use laminated glass as the inner layer. In the event of damage to one of the glass panes, an adhesive layer will hold the glass shards.

Glass beams support the glass panels with mechanical or adhesive connections [56, 59]. Mechanical connections are represented by metal clamp fixings (linear or point support), drilled fixings and other metal connectors. Mechanical point supports provide fully rigid restraint to the joined glass panels, allowing the minimisation of the metal substructures. Adhesive connections are continuous within the connections of the glass panel to the glass beam. Two different types of structural silicone sealants are available, namely one- and two-component silicones [26]. Under loads applied to the glass panels, the adhesive joint behaves as a rigid joint in the z-direction, while the same connection works as a flexible shear connection toward the possible out-of-plane direction (y-direction) [56].

4.2. Case study of historical buildings with steel-glass roofs

Currently, solutions for roof coverings that combine load-bearing steel and glass elements are uncommon. However, existing implementations in this area can make an important contribution to the consideration on how to design such roofing into the historic fabric. One example of such solutions is provided by the Senate House in London. The building was erected for the university in the 1930s. It was designed by Charles Holden. The building was designed in the art-deco style and constituted the first phase of an unfinished university complex. It consists of 19 floors and is 64 m high. At the time of its construction, it was the tallest building in London [67], following St Paul's Cathedral. In 1969, Senate House was entered on the list of monuments in the UK as a Grade II monument.

The contemporary challenges of higher education development prompted the decision to refurbish and extend the building. The architectural proposition was prepared by Rock Townsend Architects. The design activities were aimed at providing additional space for students to study, meet and relax. The new student centre was located in the northern block on the lower ground floor and the ground floor, which replaced a formerly unused internal courtyard. A glass roof was designed above the courtyard at the first-floor level. Its plan measures 27.9 × 21.0 m. The roof is supported by eight internal columns so as not to strain the existing masonry structures. Its carved form is a characteristic feature of the structure. The main roof structure consists of curved steel beams (Figure 6) with a span of 15 m. The cross-section of the beams was designed as a welded trapezoidal shape. The glass beams are 3 m long and have been arranged perpendicularly and placed every 1.5 m. Their cross-section measures 48.56 × 250 mm. The beams were designed of four layers of heat-strengthened glass, bonded with 1.52 mm PVB film. The inner layers of glass are 12 mm thick, while the outer layers are 10 mm thick. The beams support a glazing unit made of bent glass, whose interpane space is filled with krypton, 16 mm thick. The outer layer consists of laminated glass with two layers of 10 mm-thick float glass, bonded with a 1.52 mm-thick layer of Saflex extra stiffness film. The roof glazing is fixed to the beams with curved aluminium caps.

Steel framing systems on which the glass beams are supported can also be used in steel-glass roofs. This solution is used at Gwyn Hall in Neath. The building was built in 1887 as a Victorian theatre. It was designed by John Norton. After a fire in 2007, the building was substantially rebuilt, retaining the original façade. The architectural changes were designed by Holder Mathias Architects. As a result of the design work, the functional layout of the building was modified, and a new glass extension was designed. The main structure of the glass box consists of steel frames with a span of 5.2 m and a spacing of 4.4 m. The frames were designed with square hollow steel sections. Glass beams, 4.4 m long, were fixed perpendicular to the spacing of steel profiles. The beams act as purlins that support the glass roof panels (Figure 7). The roof glazing panels, measuring 1.50 × 2.20 m, were fixed to the glass beams using system point fixing Planar.

Steel-glass roofs can also be shaped using trusses. Trusses allow for obtaining large spans. For this reason, it was possible to design an atrium covering for the inner courtyard of the Conservatorium Hotel in Amsterdam. The building was designed by Dutch architect Daniel Knuttel and erected in a neo-Gothic style in 1901. Originally, the headquarters of the Post Office Savings Bank (Rijkspostpaarbank), it later housed the Conservatorium. The atrium was designed by MVSA Architects as part of the adaptation work to modify the building for its new use. The glass roof measures 45 × 18 m. The main structural elements of the roof consist of trusses with different spans, matching the shape of the roof and the building development within the atrium. The largest span of the steel trusses measures 18 m; they are spaced every 3.2 m. The trusses were designed as Warren trusses using rectangular hollow steel sections (Figure 8). Laminated glass beams 3.2 m long are attached to the trusses to support the roof glazing.

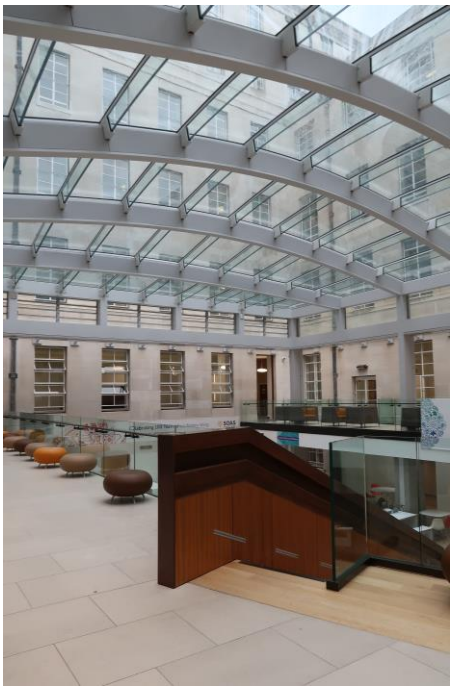

Fig. 6. Senate House, North Block, London, photo by Anna Jóźwik

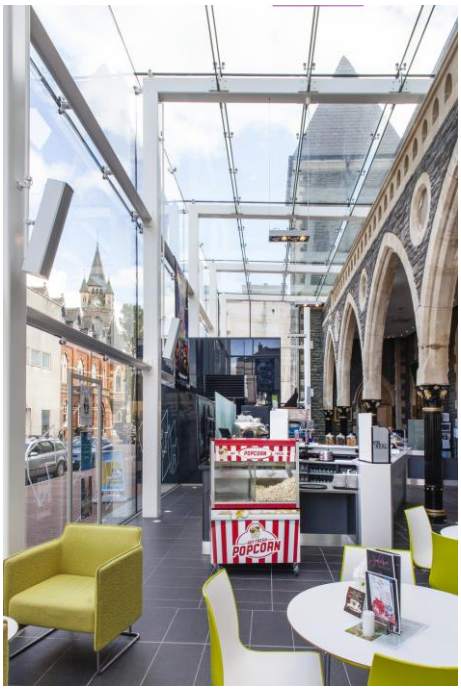

Fig. 7. Gwyn Hall, Neath, photo by ©Andrew Smith – SG Photography Ltd

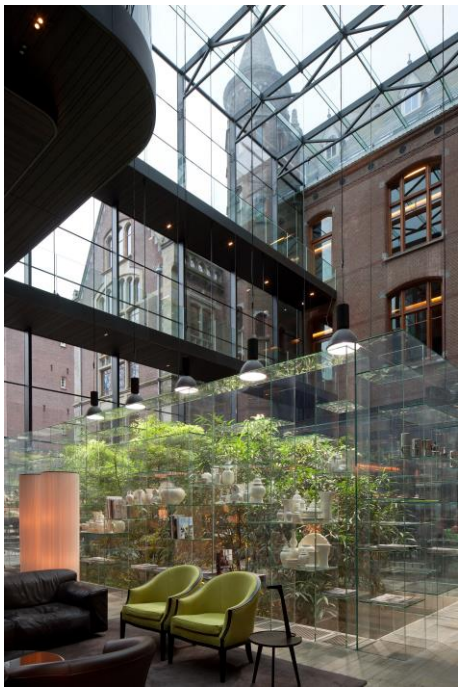

Fig. 8. Conservatorium Hotel, Amsterdam, photo by ©Amit Geron

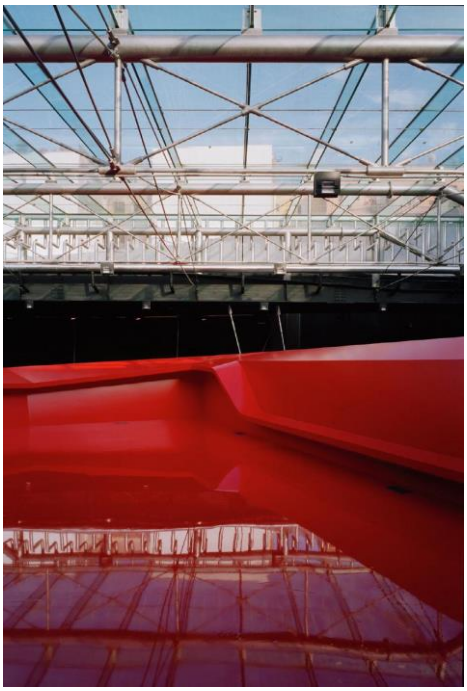

Fig. 9. Museum of Contemporary Art of Rome, Rome, photo by ©Luigi Filetici

For larger roof spans, cable structures such as cable girders or cable trusses can also be used. These offer the advantage of lightness and small cross-sections. Cable girders were used in the Macro Museum of Modern Art in Rome, which was built on the site of the former Peroni brewery. The new utility function in the post-industrial area involved an extension of the facility. The architectural design by Studio Odile Decq assumed that, under the adaptation of the area of the 19th-century Peroni Brewery, the additional development of a substantial area centred around a central atrium would be conducted. The building's glazed roof, on a polygonal plan, acts as a skylight. The main structural elements include x-shaped lattice girders (Figure 9), with a top chord of circular hollow sections. The girders have a maximum span of 18 m and are spaced every 2.5 m. The 2.5 m long glass beams were fixed by steel consoles welded to the top chord of the girders. In addition, glass beams perpendicular to the purlins were used in the axes of the top chord, thus creating a grid system.

5. CONCLUSION

Adaptive reuse can be an effective strategy for the preservation of cultural heritage, as it takes into account various aspects, such as architectural, technical, economic, and sustainability issues. The neutral perception of glass offers great opportunities in adaptive design solutions. Glass can be used to shape roof coverings in existing buildings over internal courtyards, extensions and links. Structurally, steel-glass roofs using glass beams are one of the possible solutions. Glass beams, despite being second-order elements in these load-bearing systems, attract attention to their design methods. A significant problem is posed by the phenomenon of lateral-torsional buckling, which results from the geometrical conditions of the beam and the slenderness ratio of the cross-section. Several approaches have been developed to determine critical moment values for lateral-torsional buckling. One of the key issues in the design of glass beams as composite elements is determining the equivalent thickness, i.e. the thickness in bending and compression. The effective thickness value depends on the mechanical and geometrical properties of both the glass layers and the interlayers, as well as the conditions of loading and edge conditions [68]. In the works available to date [43–46], references can be found to the sandwich theory described by Stamm and Witte [42] and the Bennison-Wöfel method [69, 70]. Currently, the Enhanced Effective Thickness (EET) method [71–73] is used to determine the thickness in bent element sections, which can be seen as an improvement in comparison to the Bennsion-Wöfel method. The Enhanced Effective Thickness method is based on the hypothesis of small deformations and the role of the interlayer is limited to the transmission of shear between glass layers and is and is characterised by the degree of bonding of the layers. The degree of bonding in laminated glass is determined by the η coefficient. Its value ranges from 0 to 1, with $\eta = 0$ indicating no bonding, $\eta = 1$ full bonding [20]. Additionally, due to the degree of shear bonding of the glass layers by the interlayer, the Enhanced Effective Thickness (EET) for torsion has been derived [74].

The glass beam design method is included in the normative documents: the Australian Standard AS1288 [75], the Guide for the Design, Construction and Control of Buildings with Structural Glass Elements [51] and the Technical Specification CEN/TS 19100 [76], which is a preview of the future Eurocode 10. Part three of the CEN/TS 19100 provides guidelines for the equivalent imperfection to be applied when verifying elements subjected to in-plane loading, for the occurring stability phenomena. The committee developing the future Eurocode CEN/TC250/SC11 has already identified a range of corrections and supplements, among which buckling curves for flexural and lateral-torsional buckling and their combinations for simple load cases and simple aspect formats of glass panes [21] can be found. The development of the Eurocode for the design of structural glass, including the design of glass beams, will make verification using numerical methods unnecessary in simple design cases. It will thus make it

possible to design load-bearing structures with glass beams more widely, also for the adaptive reuse of historic buildings.

REFERENCES

1. Robert, P 1989. *Adaptations. New Uses for Old Buildings*. Paris: Editions du Moniteur.
2. Szmygin, B (ed) 2009. *Adaptacja obiektów zabytkowych do współczesnych funkcji użytkowych [Adaptation of historic buildings to modern utility functions]*. Lublin: Wydawnictwo Politechniki Lubelskiej.
3. Bullen, PA and Love, PED 2011. Adaptive reuse of heritage buildings. *Structural Survey* **29(5)**, 411–421.
4. Misirlisoy, D and Günçe, K 2016. Adaptive reuse strategies for heritage buildings: A holistic approach. *Sustainable Cities and Society* **26**, 9198.
5. Plevoets, B and Van Cleempoel, K 2019. *Adaptive Reuse of the Built Heritage. Concepts and Cases of an Emerging Discipline*. London: Routledge.
6. Pintossi, N, Kaya, DI, Van Wesemael, P, Roders, AP 2023. Challenges of cultural heritage adaptive reuse: A stakeholders-based comparative study in three European cities. *Habitat International* **136**, 102807.
7. Stone, S 2023. Notes towards a definition of adaptive reuse. *Architecture* **3**, 477–489.
8. Wilkinson, SJ, Remøy, H and Langston C 2014. *Sustainable Building Adaptation: Innovations in Decision-making*. Oxford: Wiley Blackwell.
9. Vafaie, F, Remøy, H and Gruis, V 2023. Adaptive reuse of heritage buildings; a systematic literature review of success factors. *Habitat International* **142**, 102926.
10. ICOMOS New Zealand Charter for the Conservation of Places of Cultural Heritage Value. NZ ICOMOS – ICOMOS: Auckland, New Zealand, 2010.
11. Douglas, J 2006. *Building Adaptation.* London: Routledge.
12. Plevoets, B and Van Cleempoel, K 2011. Adaptive reuse as a strategy towards conservation of cultural heritage: a literature review. In: Brebbia, CA and Binda, L (ed) *Structural Studies, Repair and Maintenance of Heritage Architecture XII*. Southampton: WIT Press, 155–164.
13. Plevoets, B and Van Cleempoel, K. 2013. Adaptive reuse as an emerging discipline: an historic survey. In: Cairns G (ed), *Reinventing Architecture And Interiors: A Socio-Political View on Building Adaptation*. London: Libri Publishers, 13–32.
14. Nevzat, MZ, Atakara, C 2015. A contemporary connection to historic buildings through transparency and reusability. *Open House International* **40(3)**, 52–60.
15. Smilde, JA 2016. *Transparent restoration of a historic building using structural glass elements*. Master thesis. Delf: Delft University of Technology.
16. Jóźwik, A 2018. Szkło konstrukcyjne w modernizacji obiektów zabytkowych [Structural glass in modernization of hertitage buildings]. *Inżyniera i Budownictwo* **74(4)**, 173–177.
17. Jóźwik, A 2022. Application of glass structures in architectural shaping of all-glass pavilions, extensions, and links. *Buildings* **12(8)**, 1254.
18. Bekar, I and Kutlu, İ 2022. Glass use in re-used historical buildings: The case study of Trabzon Kizlar Monastery. *International Journal of Conservation Science* **13(4)**, 1129–1142.
19. Jäger, FP 2010. *Old & New—Design Manual for Revitalizing Existing Buildings* Old & New—Design Manual for Revitalizing Existing Buildings. Basel: Birkhäuser.
20. Jóźwik, A 2022. Introduction to structural design of glass according to current European standards. *Archives of Civil Engineering* **68(2)**, 147–170.

21. Feldmann, M, Laurs, M, Belis, J et al. 2023. The new CEN/TS 19100: Design of glass structures. *Glass Structures Engineering* **8**, 317–337.
22. EN 572-1:2012+A1:2016 Glass in building—Basic soda-lime silicate glass products. Part 1: Definitions and general physical and mechanical properties.
23. EN 1999-1-1:2007/A1:2009 Eurocode 9: Design of aluminium structures. Part 1-1: General structural rules.
24. EN 1993-1-1:2005/A1:2014 Eurocode 3: Design of steel structures. Part 1-1: General rules and rules for buildings.
25. Feldmann, M, Kasper, R and at al. 2014. *Guidance for European Structural Design of Glass Components*. Luxembourg: Publications Office of the European Union.
26. Haldimann, M, Lubile and Overend, M 2008. *Structural Use of Glass*. Zürich: IABSE.
27. Griffith, AA 1921. The phenomena of rupture and flow in solids. *Philosophical Transactions of the Royal Society of London. Series A, Containing Papers of a Mathematical or Physical Character* **221**, 163–198.
28. EN 12150-1:2015+A1:2019 Glass in building—Thermally toughened soda lime silicate safety glass - Part 1: Definition and description.
29. EN 14179-1:2016 Glass in building—Heat soaked thermally toughened soda lime silicate safety glass - Part 1: Definition and description.
30. EN 1863-1:2011 Glass in building—Heat strengthened soda lime silicate glass. Part 1: Definition and description.
31. EN 12337-1:2000 Glass in building—Chemically strengthened soda lime silicate glass. Part 1: Definition and description.
32. CEN/TS 19100-1:2021 Design of glass structures. Part 1: Basis of design and materials.
33. Bedon, C, Amadio, C and Noè, S 2019. Safety Issues in the Seismic Design of Secondary Frameless Glass Structures. *Safety* **5(4)**, 80.
34. EN 16612:2019 Glass in building—Determination of the lateral load resistance of glass panes by calculation.
35. Kosmal, M, Kuśnierz, A and Kozłowski, M 2022. *Szkło Budowlane [Building Glass]*. Warsaw: Wydawnictwo Naukowe PWN.
36. Pelfrene, J, Van Dam, S, Spronk, S and Van Paepegem, W 2018. *Experimental Characterization and Finite Element Modelling of Strain-rate Dependent Hyperelastic Properties of PVB Interlayers*. Challenging Glass 6 – Conference on Architectural and Structural Applications of Glass, Delf, The Netherlands, 17–18 May 2018.
37. Martin, M et al. 2022. Polymeric interlayer materials for laminated glass: A review. *Construction and Building Materials* **230**, 116897.
38. Bos, FP 2009. *Safety Concepts in Structural Glass Engineering: Towards an Integrated Approach*. Doctoral thesis. Delf: Delft University of Technology.
39. Kozłowski, M 2019. *Balustrady Szklane. Analizy Doświadczalne i Obliczeniowe, Podstawy Projektowania [Glass Balustrades: Experimental And Numerical Analysis, Basis of Design]*. Gliwice: Wydawnictwo Politechniki Śląskiej.
40. Bennison, SJ, Jagota, A and Smith CA 1999. Fracture of glass/poly(vinyl butyral) (Butacite (R)) laminates in biaxial flexure. *Journal of the American Ceramic Society*, **82**, 1761–1770.
41. Kott, A and Vogel, T 2006. Safety of laminated glass structures after initial failure. *Structural Engineering International* **14(2)**, 134–138.
42. Stamm, K and Witte, H 1974. *Sandwichkonstruktionen. Berechnung, Fertigung, Ausfüh*rung. Wien: Springer-Verlag.

43. Luible, A 2004. *Stabilität von Tragelementen aus Glas [Stability of load carrying elements of glass]*. Thèse EPFL 3014. Lausanne: Ecole Polytechnique Fédérale de Lausanne (EPFL).
44. Lubile, A and Crisinel, M 2006. *Lateral torsional buckling of glass beams*. Progress in Steel, Composite and Aluminium Structures. Proceedings of the XI International Conference on Metal Structures (ICMS 2006), Rzeszow, Poland, 21–23 June 2005, 971–978.
45. Luible, A and Crisinel, M 2006. *Design of glass beams subjected to lateral torsional buckling*. IABSE Symposium 'Responding to Tomorrow's Challenges in Structural Engineering', Report n. 92; Budapest, Hungary; IABSE—International Association for Bridge and Structural Engineering: Zurich, Switzerland, 2006, 45–53.
46. Amadio, C and Bedon, C 2010. Buckling of laminated glass elements in out-of-plane bending. *Engineering Structures* **32(11)**, 3780–3788.
47. Belis, J et al. 2013. Experimental and analytical assessment of lateral torsional buckling of laminated glass beams. *Engineering Structures* **51**, 295–305.
48. Bedon, C, Belis, J and Luible, A 2014. Assessment of existing analytical models for the lateral torsional buckling analysis of PVB and SG laminated glass beams via viscoelastic simulations and experiments. *Engineering Structures* **60**, 52–67.
49. Bedon, C and Amadio, C 2015. Design buckling curves for glass columns and beams. *ICE Proceedings Structures and Buildings* **168(7)**, 514–526.
50. Pešek, O and Melcher, J 2017. Lateral-torsional buckling of laminated structural glass beams. experimental study. *Procedia Engineering* **190**, 70–77.
51. CNR-DT 210/2013 Guide for the Design, Construction and Control of Buildings with Structural Glass Elements.
52. Ferreira, GNA 2022. Design of multi-layered laminated glass beams in lateral-torsional buckling. *International Journal of Structural Glass and Advanced Materials Research* **6(1)**, 23–32.
53. Belis, J and Bedon C 2014. Strengthening effect of structural sealants on the LTB behavior of glass beams. In: Louter, L, Bos, F, Belis, J and Lebet JP (ed) *Challenging Glass 4 & COST Action TU0905 Final Conference*. Leiden: CRC Press/Balkema, 671–680.
54. Bedon C and Amadio, C 2015. Analytical and numerical assessment of the strengthening effect of structural sealant joints for the prediction of the LTB critical moment in laterally restrained glass beams. *Materials and Structures* **49**, 2471–2492.
55. Bedon, C, Belis, J and Amadio, C 2015. Structural assessment and lateral-torsional buckling design of glass beams restrained by continuous sealant joints. *Engineering Structures* **102**, 214–229.
56. Bedon, C and Belis, J 2016. Mechanical behavior and resistance of structural glass beams in lateral-torsional buckling (LTB) with adhesive joints. In: Tiwari, A, Murugan AN, and Ahuja, R (ed) *Advanced Engineering Materials and Modeling*. Beverly: Scrivener Publishing/Wiley, 3–47.
57. Luible, A and Schärer, D 2016. Lateral torsional buckling of glass beams with continuous lateral support. *Glass Structures & Engineering* **1**, 153–171.
58. Sonck, D and Belis, J 2016. Elastic lateral-torsional buckling of glass beams with continuous lateral restraints. *Glass Structures & Engineering* **1**, 173–194.
59. Santo, D, Mattei, S and Bedon, C 2020. Elastic critical moment for the lateral-torsional buckling (LTB) analysis of structural glass beams with discrete mechanical lateral restraints. *Materials* **13(11)**, 2492.
60. Causevic, A, Salihbegovic, A and Rustempasic, N 2018. *Integrating New Structures with Historical Constructions – A Transparent Roof Structure above the Centrally Designed Atrium*. 3rd World Multidisciplinary Civil Engineering, Architecture, Urban Planning Symposium (WMCAUS 2018), Prague, Czech Republic, 18–22 June 2018; IOP Conference Series Materials Science and Engineering **471**, 112102.

61. Żółtowski, W and Łubiński, M 2007. *Konstrukcje metalowe. Obiekty budowlane. Część 2. [Steel Constructions. Buildings. Part 2]*. Warsaw: Arkady.
62. Żmuda, J 2016. Projektowanie konstrukcji stalowych. *Część 1. Dźwigary kratownicowe, słupy, ramownice [Design of steel structures. Part 1. Truss girders, columns, frames]*. Warsaw: PWN.
63. Majowiecki, M 1971. Tension Structures: Jawerth System. *Acier/Stahl/Steel* **4**, 169–177.
64. Kocur, R 2023. Szklane konstrukcje cięgnowe na Muzeum i Centrum Ruchu Harcerskiego w Krakowie. Część 1 – Koncepcja konstrukcyjna [Glass tension structures for the Museum and Center of the Scout Movement in Krakow. Part 1—Structural concept]. *Świat Szkła* **6**, 10–16.
65. Saitoh. M and Okada A 1999. The role of string in hybrid string structure. *Engineering Structures* **21,** 756-769.
66. Bijster, J, Noteboom, C. and Eekhout, M 2016. Glass entrance Van Gogh Museum Amsterdam. *Glass Structures & Engineering* **1**, 205–231.
67. Boyd, J 2013. Senate House Tower—the capital's first skyscraper. *The London Journal* **33**, 249–269.
68. Green R, Bedon, C and Galuppi, L 2023. Design and stability of laminated glass fins with continuous lateral silicone restraint. *Glass Structures & Engineering* **8**, 363-382.
69. Wölfel, E 1987. Nachgiebiger Verbund Eine Näherungslösung und deren Anwendungsmöglichkeiten [Elastic bond: an approximate solution and its applications]. *Stahlbau* **6**, 173–180.
70. Bennison SJ, Stelzer I 2009. *Structural properties of laminated glass. In: Short Course*. Glass Performance Days, Tampere, Finland, 12–15 June 2009.
71. Galuppi, L and Royer-Carfagni, G 2012. Effective thickness of laminated glass beams: New expression via a variational approach. *Engineering Structures* **38**, 53–67.
72. Galuppi, L, Manara, G and Royer-Carfagni, G 2013. Practical expressions for the design of laminated glass. *Composites Part B: Engineering* **14(1)**, 1677–1688.
73. Galuppi, L and Royer-Carfagni, G 2014. Enhanced Effective Thickness of multi-layered laminated glass. *Composites Part B: Engineering* **64**, 202–213.
74. Galuppi, L and Royer-Carfagni, G 2020. Enhanced Effective Thickness for laminated glass beams and plates under torsion. *Engineering Structures* **206**, 110077.
75. AS1288:2006 Glass in Buildings—Selection and Installation.
76. CEN/TS 19100-3:2021 Design of glass structures. Part 3: Design of in-plane loaded glass components and their mechanical joints.